

## RESEARCH ARTICLE

# Inhibition of glioblastoma proliferation, invasion, and migration by Urolithin B through inducing G0/G1 arrest and targeting MMP-2/-9 expression and activity

Fateme Eidizade<sup>1</sup>  | Mohammad Soukhtanloo<sup>1,2,3</sup> | Rahele Zhiani<sup>4,5</sup> |  
Jamshid Mehrzad<sup>1</sup> | Farshad Mirzavi<sup>6</sup>

<sup>1</sup>Department of Biochemistry, Neyshabur Branch, Islamic Azad University, Neyshabur, Iran

<sup>2</sup>Department of Clinical Biochemistry, Faculty of Medicine, Mashhad University of Medical Sciences, Mashhad, Iran

<sup>3</sup>Pharmacological Research Center of Medicinal Plants, Mashhad University of Medical Sciences, Mashhad, Iran

<sup>4</sup>Department of Chemistry, Neyshabur Branch, Islamic Azad University, Neyshabur, Iran

<sup>5</sup>New Materials Technology and Processing Research Center, Department of Chemistry, Neyshabur Branch, Islamic Azad University, Neyshabur, Iran

<sup>6</sup>Cardiovascular Diseases Research Center, Birjand University of Medical Sciences, Birjand, Iran

## Correspondence

Mohammad Soukhtanloo, Department of Biochemistry, Neyshabur Branch, Islamic Azad University, Neyshabur, Iran.  
Email: [soukhtanloom@mums.ac.ir](mailto:soukhtanloom@mums.ac.ir)

Rahele Zhiani, Department of Chemistry, Neyshabur Branch, Islamic Azad University, Neyshabur, Iran.  
Email: [r\\_zhiani2006@yahoo.com](mailto:r_zhiani2006@yahoo.com)

## Abstract

One kind of brain cancer with a dismal prognosis is called glioblastoma multiforme (GBM) due to its high growth rate and widespread tumor cell invasion into various areas of the brain. To improve therapeutic approaches, the objective of this research investigates the cytotoxic, anti-metastatic, and apoptotic effect of urolithin-B (UB) as a bioactive metabolite of ellagitannins (ETs) on GBM U87 cells. The malignant GBM cell line (U87) was examined for apoptosis rate, cell cycle analysis, cell viability, mRNA expressions of several apoptotic and metastasis-associated genes, production of reactive oxygen species (ROS), MMP-2, and MMP-9 activity and protein expression, and migration ability. The findings revealed that UB decreased U87 GBM viability in a dose-dependent manner and NIH/3T3 normal cells with the IC<sub>50</sub> value of 30 and 55 μM after 24 h, respectively. UB also induces necrosis and G0/G1 cell cycle arrest in U87 cells. UB also increases ROS production and caused down-regulation of Bcl2 and up-regulation of Bax apoptotic genes. Additionally, treatment of UB reduced the migration of U87 cells. The protein levels, mRNA expression, and the MMP-2 and MMP-9 enzyme activities also decreased concentration-dependently. So, due to the non-toxic nature of UB and its ability to induce apoptosis and reduce the U87 GBM cell invasion and migration, after more research, it can be regarded as a promising new anti-GBM compound.

## KEYWORDS

glioblastoma multiform, invasion, matrix metalloproteinase, migration, urolithin B

## 1 | INTRODUCTION

One kind of brain cancer with a dismal prognosis is called glioblastoma multiforme (GBM). The tumor

originates from astrocyte glial cells and is extremely dangerous due to the fast proliferation and infiltration of tumor cells into various areas of the brain.<sup>1</sup> Surgery to remove the tumor is always difficult due to glioblastoma's

**List of Abbreviations:** AB, Alamar Blue; BCA, bicinchoninic acid; DCFDA, dichloro-dihydro-fluorescein diacetate; DMEM, Dulbecco's modified Eagle's medium; EA, ellagic acid; ECM, extracellular matrix; ETs, ellagitannins; FBS, Fetal bovine serum; GBM, glioblastoma multiforme; HIF, hypoxia-inducible factor; JNKs, c-Jun N-terminal kinases; MMPs, matrix metalloproteinases; MPTP, mitochondrial permeability transition pore; NAC, N-acetyl-cysteine; ROS, reactive oxygen species; TBS, Tris-buffered saline; UA, urolithin-A; UB, Urolithin-B; VEGFR, VEGF-receptor.

aggressive nature. The existing treatment such as tumor surgery, radiation therapy, or chemotherapy (Temozolomide, etc.) is not too effective in increasing the average survival rate of 12–15 months.<sup>2,3</sup> Therefore, to improve the therapeutic approach, antitumor agents that target GBM cancer cell proliferation and metastasis are needed.

Natural product research is an effective method for identifying biologically active substances and has been crucial in discovering novel structures and mechanisms of action that may be utilized to treat a variety of human illnesses. Numerous natural compounds, notably those used in the treatment of cancer like Taxol, Metformin, Vinblastine, and Camptothecin, are now undergoing clinical testing.<sup>4,5</sup>

Both ellagitannins (ETs) and ellagic acid (EA) have shown potential preventive effects against different types of diseases including diabetes, neurodegenerative diseases, and cancer via their anti-inflammatory, antioxidant, estrogenic modulators, and anticarcinogenic effects.<sup>6</sup> Pomegranate, walnut, strawberry, and many other nuts and fruits are rich in active compounds ET and EA. The bioavailability and metabolism of ET and EA are very low and unabsorbed compounds metabolized to bioavailable products urolithin-A (UA, 3,8-dihydroxy-6*H*-dibenzo[*b,d*] pyran-6-one) and urolithin-B (UB, 3-hydroxy-6*H*-dibenzo[*b,d*] pyran-6-one) (Figure 1). After urolithins production and absorption into the bloodstream metabolized again and conjugated with methyl, glucuronic acid, or sulfate that can persist in the blood up to 3–4 days after the intake. Consistently, various types of studies showed that the main metabolites in plasma after consumption of ET-containing foods are UA and UB in different animals and humans.<sup>7</sup> UA as well as UB were detected in the animal's brain after intravascular and oral administration and showed neuroprotective effects in Alzheimer's

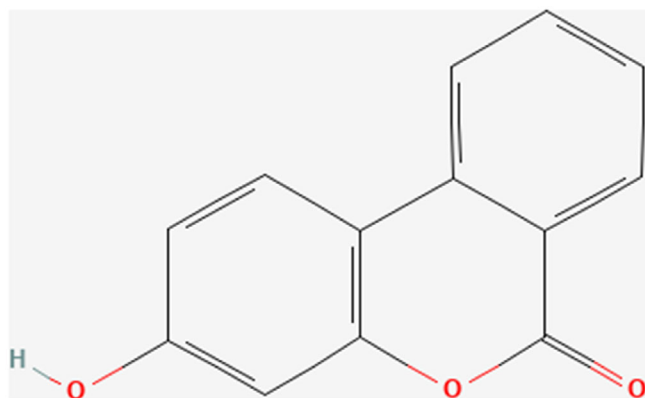


FIGURE 1 Chemical structure of UB 3-hydroxy-6*H*-dibenzo[*b,d*] pyran-6-one (molecular weight 212.20 g/mol). UB, urolithin B

and Parkinson's animal models.<sup>8–12</sup> In addition, different in vitro studies conducted with urolithins on neuronal cell models concluded that using physiologically concentrations (up to 10  $\mu$ M) of the free and conjugated form of UB as well as UA can exert a high neuroprotective effect mediated through the prevention of neuronal apoptosis, anti-oxidant, and anti-inflammatory activities.<sup>12</sup> However, some other in vitro studies have evaluated and compared the neuroprotective effect of UB with its circulating conjugated forms reporting lower attenuation on the H<sub>2</sub>O<sub>2</sub>-induced cytotoxicity in neuroblastoma SH-SY5Y cells.<sup>13,14</sup> Moreover, recent studies revealed that UB can reduce metastasis and induce apoptosis in varied types of cancerous cells such as prostate, bladder, breast, and colon.<sup>15–18</sup> Considering that UB could reach the brain and its anticancer effect, it may be considered a potential candidate for GBM therapy. But molecular, cellular, and metabolic mechanisms related to cytotoxic and anti-metastatic behavior of UB on GBM cells remain to be determined. All things considered, this research study aimed to evaluate UB's cytotoxic and anti-metastatic effects on GBM cancer cells for the first time.

## 2 | MATERIAL AND METHODS

### 2.1 | Chemical reagents

Propidium iodide (PI), penicillin–streptomycin, and Resazurin powder were provided from Sigma–Aldrich. High-glucose Dulbecco's Modified Eagle's Medium (DMEM), trypsin–EDTA, and Fetal bovine serum (FBS) were acquired from Gibco. The dichloro-dihydro-fluorescein diacetate (DCFDA)/H2DCFDA-cellular ROS detection assay kit was obtained from Abcam. *N*-Acetylcysteine (NAC) and Annexin V-FITC assay kit were bought from Cayman Chemical. Specific antibodies against beta-actin, MMP-2, and MMP-9 were prepared from Zell BIO GmbH. The secondary antibody horseradish peroxidase-conjugated was obtained from (Santa Cruz). The SuperSignal<sup>®</sup> chemiluminescence kit was obtained from Thermo Fisher Scientific, Inc. The bicinchoninic acid (BCA), kit for protein assays, was acquired from Pars Tous. UB was provided by Golexir Pars Co. Unless otherwise provided, all additional compounds were bought from Sigma–Aldrich.

### 2.2 | Cell culture

The malignant glioblastoma multiform cell line Uppsala 87 (U87) and the non-neoplastic NIH/3T3 fibroblast cell

line were provided by Iran's National Cell Bank (Pasteur Institute). The cells were cultured in high glucose DMEM complemented with 100 unit/ml of penicillin–streptomycin and 10% FBS.

### 2.3 | Cell viability assay

Cytotoxicity was determined based on the colorimetric Alamar Blue (AB) assay. AB contained a redox dye named resazurin, which metabolically active cells reduced to resorufin and dihydro resorufin measured by both colorimetric and fluorometric changes.<sup>19</sup> Briefly, in 96 well plates ( $1.2 \times 10^4$  cells/well), U87 and NIH/3T3 cells were seeded and incubated for a whole night at 37°C with 5% CO<sub>2</sub>. Then, the U87 cells were treated with various doses of UB (4.68, 9.37, 18.75, 37.5, 75, 150, 300, and 600 μM) for 24 h. Next, after adding AB (0.01 mg/mL of resazurin dissolved in PBS) to each well for 3 h, the fluorescence was measured (530/590 nm) using a Victor X5 Multiplable Plate Reader (Perkin Elmer). All the treatments were performed in triplicate. The IC<sub>50</sub> value was determined using GraphPad Prism<sup>®</sup> 8.2.1 software.

### 2.4 | Cell cycle analysis

U87 cells were seeded in 6-well plates ( $10^5$  per well) and were incubated with 30 μM of UB for 24 h. Following trypsinization, cells were fixed in 70% ethanol at 4°C for 2 h. Following that, at room temperature, cells were treated in PBS for 30 min with 100 mg/ml of 1% RNase. Next, 400 μl of PI solution which contains 50 μg/ml PI, 1 mg/ml sodium citrate, and 0.1% Triton X-100 was added and after 30 min of dark incubation, the cells were examined. Ten thousand cells were evaluated in each sample and cell cycle distribution was assessed in a BD FACSCALIBUR™ FLOW CYTOMETER (Becton Dickinson), and the program FlowJo V10 was used to examine the results (Flowjo).

### 2.5 | Annexin V-FITC assay

Apoptosis and necrosis of U87 cells induced by UB (30 μM) were detected using the Annexin V-FITC staining kit as described previously.<sup>20</sup> A flow cytometric assessment was carried out on 10,000 stained U87 cells using a BD FACSCALIBUR™ FLOW CYTOMETER (Becton Dickinson). The program FlowJo V10 was used to examine the results.

### 2.6 | Measurement of reactive oxygen species activity

Following the manufacturer's instructions, the cellular ROS detection kit measured the level of ROS. As described,<sup>21</sup>  $25 \times 10^3$  U87 cells were seeded and cultivated overnight into dark 96 well tissue culture plates. After overnight, the cells were washed and stained with 25 μM of H<sub>2</sub>DCFDA solution for 45 min in the dark. After rewashing, UB (15 and 30 μM) and NAC (5 Mm) were added to the cells for 24 h. A set of filters with a 485 excitation and 535 emission were used to measure the fluorescence intensity by a Victor X5 Multiplable Plate Reader. All the treatments were performed in triplicate and the results normalized to the volume of cells using the BCA protein assay method.<sup>22</sup>

### 2.7 | Quantitative real-time polymerase chain reaction (qRT-PCR)

Using the Favorgen RNA extraction kit (Favorgen Biotech), total RNA was extracted from the UB-treated U87 cells (15 and 30 μM) by the manufacturer's instructions. Utilizing agarose gel electrophoresis and UV spectrophotometry (NanoDrop 1000™), the concentration and the extracted RNA's purity were evaluated. Total RNA was reverse transcribed to cDNA using an easy cDNA synthesis kit (Parstous), and qRT-PCR with specific primers for GAPDH, Bax, Bcl-2, VEGF, MMP-2, MMP-9, and VEGFR listed in Table 1 (Metabion) was done using RealQ Plus 2X-MasterMix Green without Rox™ (Amplicon) and a Light-Cycler 96 real-time PCR system was used for the amplification (Roche). The relative expression of genes was evaluated using the Livak technique.

### 2.8 | Gelatine zymography

The gelatinolytic activities and secretion of two members of matrix metalloproteinase (MMP-9 and -2) were evaluated by gelatine zymography as described before.<sup>23,24</sup> In brief, the U87 cells were treated with UB (15 and 30 μM) for 24 h. After centrifuging the culture media, 30 μg of total protein were electrophoresed on an SDS polyacrylamide gel at a concentration of 12% with 0.1 mg/ml gelatine as a substrate. The gel was washed using 2% Triton X-100 three times for 60 min to remove SDS. Then, the gel was incubated for 48 h to allow the gelatine to be digested at 37°C in an incubation buffer containing 2.5% Triton X-100, 50 mM Tris pH 7.4, 5 mM CaCl<sub>2</sub>, and 1 μM ZnCl<sub>2</sub>. In the next step, for staining the gel used 0.5%

TABLE 1 The sequence of primers

Gene symbol	Gene name	Primers (5' → 3')	Accession number
Bax	Bcl-2-associated X protein	Forward: TGACGGCAACTTCAACTGGG Reverse: CTTCAGTGA CTGCCAGGG	NM_001291428.2
Bcl-2	B-cell lymphoma 2	Forward: GTCATGTGTGTGGAGAGCGTC Reverse: CCGTACAGTTCACAAAGGCATC	NM_000633.3
VEGF	Vascular endothelial growth factor	Forward: AGGGCAGAATCATCACGAAGT Reverse: AGGGTCTCGATTGGATGGCA	NM_001025366.3
VEGFR	Vascular endothelial growth factor receptor	Forward: ACAATCAAGTGGTTCTGGCAC Reverse: TGTCAGCATCCAGGATAGAGG	NM_002253.4
MMP-2	Matrix metalloproteinase-2	Forward: GATACCCCTTTGACGGTAAGGA Reverse: CCTTCTCCCAAGTCCATAGC	NM_001302510.2
MMP-9	Matrix metalloproteinase-9	Forward: AGACCTGGGCAGATTCCAAAC Reverse: CGGCAAGTCTTCCGAGTAGT	NM_004994.3
GAPDH	Glyceraldehyde-3-phosphate dehydrogenase	Forward: TCAAGATCATCAGCAATGCCCTCC Reverse: GCCATCACGCCACAGTTTC	NM_001357943.2

Coomassie Brilliant Blue R-250 for 60 min and de-stained the gel with 25% ethanol plus 10% acetic acid in dH<sub>2</sub>O to see the bands. The gel was photographed using the GS-800 calibrated densitometer (Bio-Rad, HC) and images were analyzed using Image J 1.52a software (NIH).

## 2.9 | Scratch wound healing assay

To assess UB's anti-migration effectiveness, we used the Scratch wound healing test, as previously explained<sup>24</sup> briefly,  $7 \times 10^5$  U87 cells were seeded into a 6-well plate. Then a sterile 100- $\mu$ l pipette tip was used to scratch cells. Next, floating cells were removed by phosphate buffer saline (PBS). Finally, cells were incubated in a medium without serum and UB (7.5 and 15  $\mu$ M). After 24 h, using a light inverted microscope, the scratch's border regions were investigated and captured on camera (Zeiss Axiovert<sup>®</sup> 200). All the treatments were conducted in a triplicate independent test.

## 2.10 | Western blotting

Similar to earlier research, we performed western blotting to assess the expression of MMP-2 and MMP-9

proteins on UB-treated U87 cells.<sup>25,26</sup> U87 cells ( $7 \times 10^5$ ) were cultured in 6-well plates and given UB (15 and 30  $\mu$ M) treatments. Then, using a BCA protein assay kit, the protein content was determined after the cells had been lysed in RIPA lysis buffer. The lysates were transferred to nitrocellulose paper (Amersham) after being separated by 12% SDS-PAGE. After blocking with 5% skim milk mixed in Tris-buffered saline (TBS) buffer, primary antibodies were diluted (1: 1000) and were overnight incubated with the membrane. After three TBS-Tween-20 (0.1%) washes, a secondary antibody that was conjugated to horseradish peroxidase was applied to the membrane. Each protein's detection was carried out using the Super Signal<sup>®</sup> following the manufacturer's recommendation.

## 2.11 | Statistical analysis

GraphPad Prism<sup>®</sup> 8.2.1 software was used to analyze the data using a one-way analysis of variance (ANOVA) and Dunnett's post hoc test. The *p*-value <0.05 was declared to have statistical significance. Data were displayed as the mean  $\pm$  standard deviation.

## 3 | RESULTS

### 3.1 | Urolithin-B decreased the viability of U87 cells

The effect of different doses of UB (600, 300, 150, 75, 37.5, 18.75, 9.37, 4.68) on U87 GBM cells and NIH/3T3 fibroblast normal cells were investigated at 24 h using the resazurin method. As indicated in Figure 2A, UB significantly decreased the viability of U87 cells in doses higher than 37.5  $\mu\text{M}$ . The IC<sub>50</sub> value of UB on U87 cells was about 30  $\mu\text{M}$ . UB also was dose-dependently toxic to NIH/3T3 normal cells, but UB at an equivalent concentration of 37.5  $\mu\text{M}$  was not toxic for NIH/3T3 cells. Moreover, the IC<sub>50</sub> value of UB for NIH/3T3 cells was 55  $\mu\text{M}$  (Figure 2B).

### 3.2 | Urolithin-B-induced necrosis and cell cycle arrest in U87 cells

To assess the amount and mechanism of apoptosis by UB, cell cycle arrest, annexin V-FITC PI, and alteration of essential gene expression involved in the apoptotic pathway were assessed in U87 cells treated with UB. As shown in Figure 3A, the application of UB caused G<sub>0</sub>/G<sub>1</sub> phase cell cycle arrest. Moreover, the amount of apoptotic and necrotic U87 cells treated with UB was evaluated through an annexin V-FITC PI double staining kit. The results presented in Figure 3B have indicated that at a concentration of 30  $\mu\text{M}$  of UB, 14.4% of the cells were necrotic. Our results indicate that UB substantially increased necrosis in U87 cells contrasted with the control group (2.64%). Furthermore, alteration of two genes expression involved in the apoptotic pathway in U-87 cells treated with UB was evaluated using qRT-PCR. The findings revealed that the Bax pro-apoptotic and Bcl2 anti-apoptotic expression levels were remarkably and dose-dependently increased and decreased in the cells treated with UB (15 and 30  $\mu\text{M}$ ), respectively (Figure 3C).

### 3.3 | Urolithin-B increases the production of reactive oxygen species

We evaluate ROS levels by using DCFDA to evaluate ROS levels in U87 cells treated with UB (15 and 30  $\mu\text{M}$ ). The findings of the ROS assay revealed that cells treated with 30  $\mu\text{M}$  of UB had considerably higher intracellular ROS levels than control groups. NAC as a ROS inhibitor (10 mM) was used as negative control and significantly decreased ROS generation in contrast to the control group (Figure 4).

### 3.4 | Urolithin-B reduces the migration of U87 cells

The wound healing test was used to contrast the inhibitory effects of UB on U87 cell migration. According to Figure 5B, UB at concentrations of 15 and 7.5  $\mu\text{M}$ , suppressed cell migration concentration dependently. The open wound area was greater in UB treated groups compared to control untreated cells after 24 h (Figure 5A). Moreover, to explore the possible molecular target of UB involved in U87 cell motility, we looked into the expression of VEGF and VEGFR, which are necessary for the migration, metastasis, and invasion of cancerous cells.<sup>27</sup> According to Figure 5C, no noticeable change was seen in VEGF and VEGFR mRNA expression between control and UB treated U87 cells after 24 h.

### 3.5 | Urolithin-B potently reduces the activity, mRNA, and MMP-2 and MMP-9 protein expression

Since MMP-2 and MMP-9 are related to invasion, tumor relapse, and recurrence of GBM,<sup>28</sup> activity, mRNA, and MMP-2 and MMP-9 protein expression in U87 cells treated with 15 and 30  $\mu\text{M}$  of UB were evaluated. The zymography results showed that secretion and activity of MMP-2 and MMP-9 considerably decreased after treatment of U87 cells with UB (Figure 6A). MMP-2 and MMP-9 were examined by qRT-PCR and western blot on U87 cells treated with UB (15 and 30  $\mu\text{M}$ ) to determine if the decrease in mRNA expression and proteins was the cause of the reduction enzymatic activities of MMP-2 and MMP-9. According to Figure 6B, UB significantly down-regulated both MMP-2 and MMP-9 concentrations dependent on the mRNA level 24 h after treatment. In addition, UB decreased the MMP-2 and MMP-9 protein expression (Figure 6C).

## 4 | DISCUSSION

One of the clinical hallmarks of GBM is extensive tumor growth and metastasis to surrounding areas.<sup>29</sup> Research on natural products as anti-cancer agents is ongoing due to different reasons including their undesirable side effects and greater therapeutic efficiency.<sup>30</sup> The findings of the current investigation also showed that UB as a natural compound, dose-dependently decreases the viability of U87 cells with the IC<sub>50</sub> value of 30  $\mu\text{M}$ . As mentioned in the literature review, Urolithins as secondary polyphenol metabolites of EA and ETs can reduce the cell viability of tumors.<sup>31</sup>

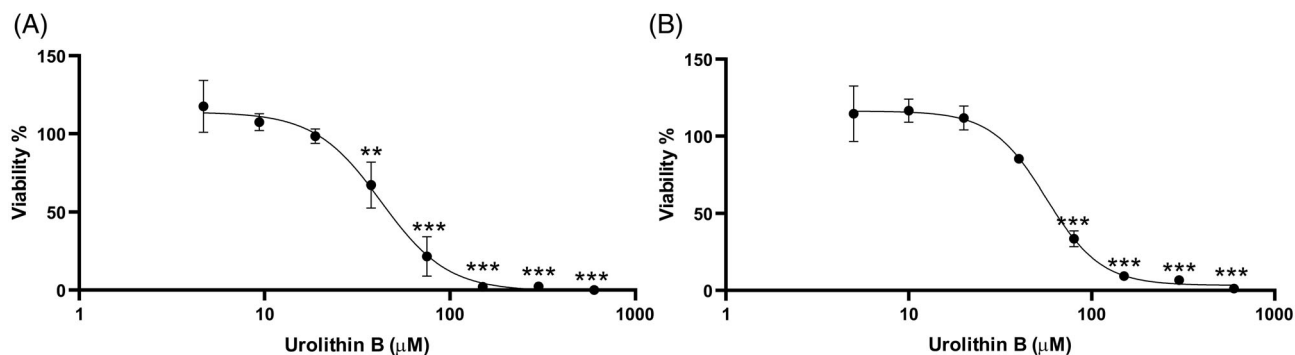


**FIGURE 2** Effects of UB at different doses on U87's cell viability (A) and NIH/3T3 (B) cells after 24 h treatment using resazurin assay. The IC<sub>50</sub> value of UB for U87 and NIH/3T3 cells was about 30 and 55  $\mu\text{M}$ , respectively. Data are an indicator of three independent investigations (mean  $\pm$  SD) (\* $p < 0.05$ , \*\* $p < 0.01$ , \*\*\* $p < 0.001$ )

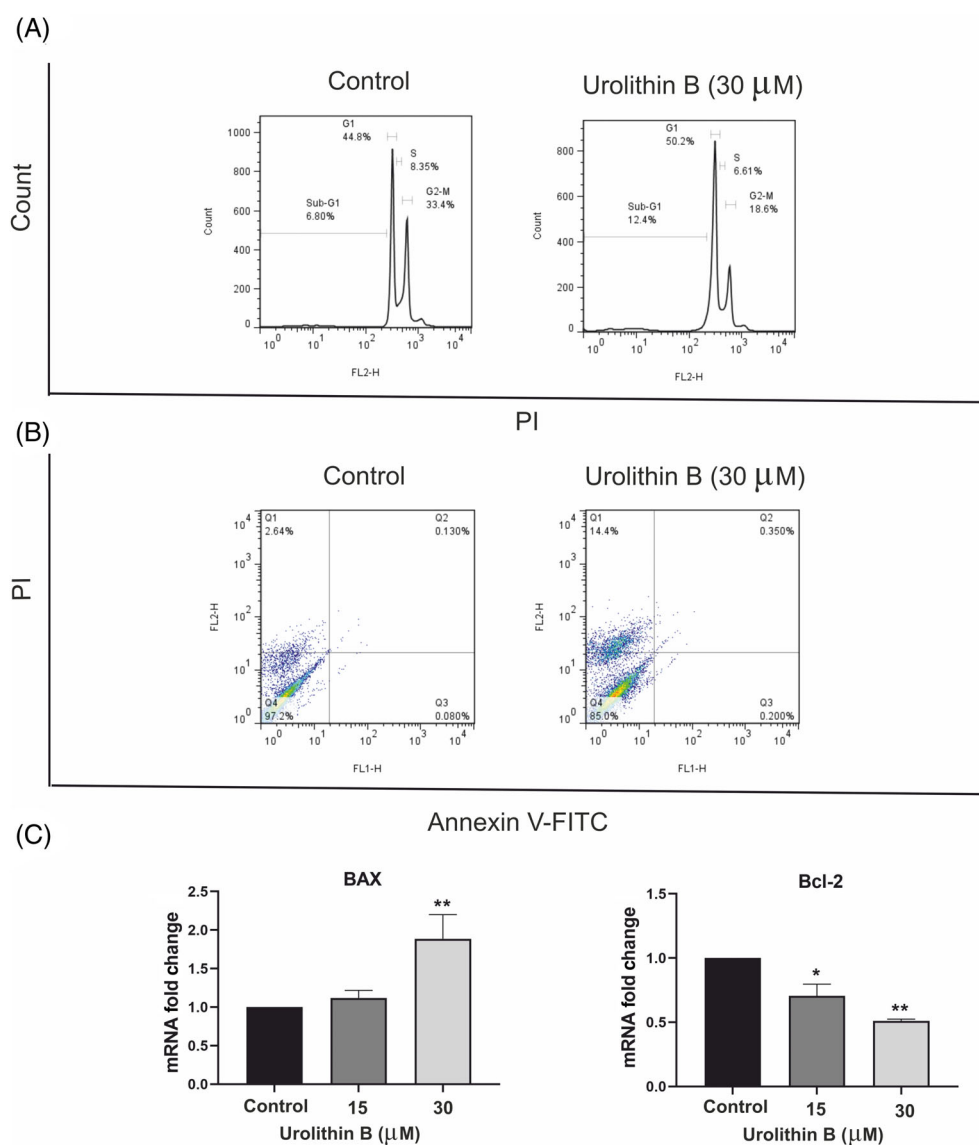


**FIGURE 3** (A) The cell cycle was assessed using flow cytometry in U87 cells stained with PI and treated with UB (30  $\mu\text{M}$ ) for 24 h. UB might considerably cause G0/G1 cell cycle arrest. X-axis and y-axis show PI and the number of U87 cells, respectively. (B) U87 GBM cells treated with UB (30  $\mu\text{M}$ ) were double-stained with Annexin V-FITC PI and evaluated with the use of flow cytometry to identify apoptosis and necrosis. U87 cells treated with UB demonstrated more necrosis than the control group. X-axis and y-axis showed annexin V-FITC and PI, respectively. Q4 to Q1 of the diagram represent live cells, early apoptotic, late apoptotic, and necrotic cells, respectively. (C) The mRNA expression of Bcl2 and Bax apoptotic genes on U87 cells treated with 15 and 30  $\mu\text{M}$  of UB was evaluated using qRT-PCR. The results are demonstrated as means  $\pm$  standard deviation (\* $p < 0.05$  and \*\* $p < 0.01$  contrasted with the control). GBM, glioblastoma multiforme; UB, urolithin B

Moreover, urolithins can induce apoptosis and reduce the proliferation of cancerous cells via cell cycle arrest, induction of necrosis, and transcriptional regulation of

apoptotic genes.<sup>31</sup> In the present research, the annexin V PI assay has also been utilized to examine the effect of UB on GBM cell apoptosis. The Annexin V PI results of

the current study showed that UB can cause necrosis induction in U87 cells. Moreover, the results of cell cycle analysis indicated the G0/G1 arrest of U87 cells treated with UB. This finding is consistent with that of Min-yi Lv (2019) indicating that UB may stop the G0/G1 cell cycle and trigger apoptosis in hepatocellular cancer cell lines.<sup>32</sup> This result may be explained by Sashi G Kasimsetty, who demonstrates various derived of ETs including Urolithins

can inhibit cell growth by inducing apoptosis during the G0/G1 and G2/M stages of the cell cycle.<sup>33</sup> Furthermore, the connection between intracellular ROS and cancer cell cycle arrest and apoptosis is well known.<sup>34</sup> The results of the present study revealed that UB can induce ROS generation at high concentrations. These results corroborate the findings of the previous work showing that UA and UB could increase the ROS level in different types of cancers.<sup>14,35</sup>

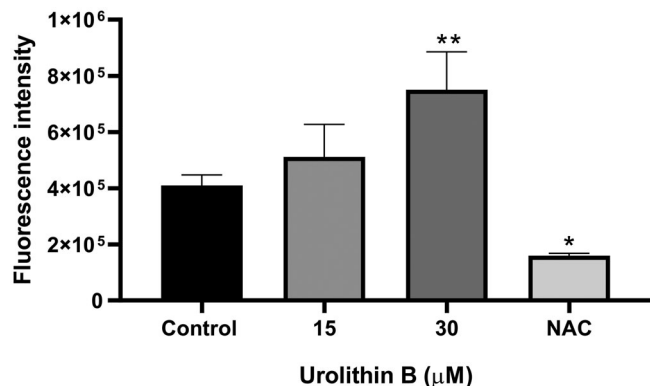


**FIGURE 4** The effect of UB on ROS generation in U87 cells after 8 h using DCFDA as a fluorogenic dye. ROS production significantly increased after 8-h treatment of U87 cells with 30 μM of UB. Also, NAC (10 mM) was applied on U87 cells as negative control and the outcomes demonstrated that ROS generation was much lower than the control. The results are expressed as means ± standard deviation (\* $p < 0.05$  and \*\* $p < 0.01$  compared to control). NAC, *N*-acetyl-cysteine; ROS, reactive oxygen species; UB, urolithin B

In response to ROS, c-Jun N-terminal kinases (JNKs) activate and alter the expression of the anti-apoptotic and apoptotic proteins.<sup>36,37</sup> One of the efficient strategies for cancer therapy is to decrease the Bcl2 family proteins that inhibit apoptosis and contribute to apoptosis resistance and increase the pro-apoptotic gene expression such as Bax.<sup>38</sup> In cancerous cells, Bcl2 bind to Bax reduced pore formation and cytochrome c release, and inhibits intrinsic apoptosis.<sup>39</sup> According to the study's findings, the U87 cells treated with UB enhanced the expression of the pro-apoptotic protein Bax and decreased the expression of the anti-apoptotic protein Bcl-2. These outcomes are in line with those of Min-yi Lv et al., who discovered that UB can significantly reduce the expression of Bcl-2.<sup>14</sup> Moreover, previous research on the anti-cancer properties of UA, another analog of a metabolite of the EA, decreases expression in Bcl-2/Bax ratio.<sup>35,40</sup> However, the results of the Annexin V-FITC showed that cytotoxicity of UB is mediated only by necrosis induction and cell cycle arrest not by apoptosis. Different types of studies reported that necrosis is not just an accidental form of cell death and

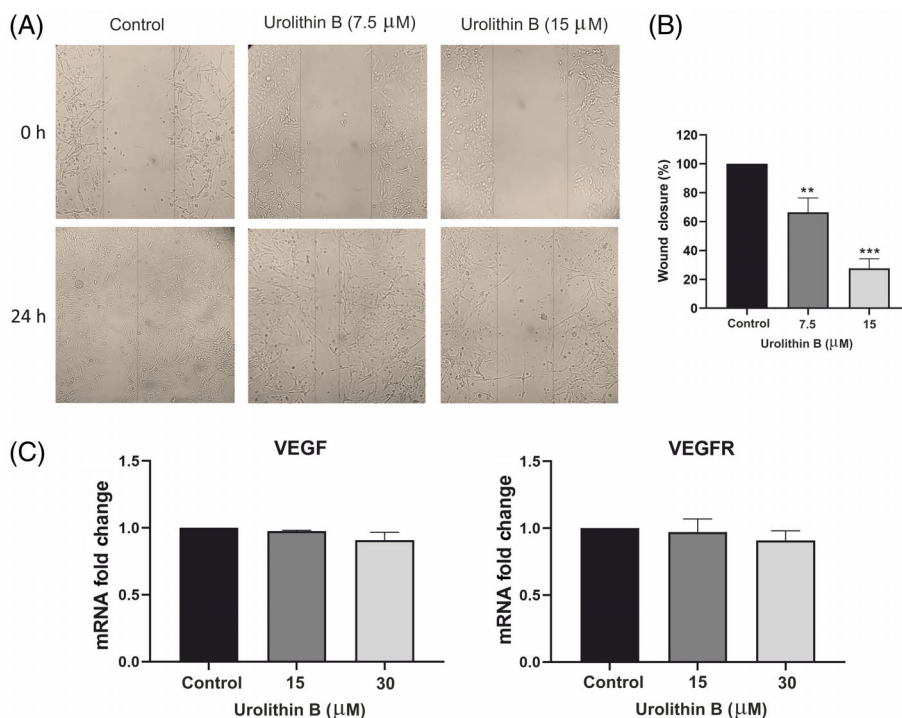


**FIGURE 5** (A) Effect of UB (7.5 and 15 μM), employing a wound healing approach, on the migration of U87 cells. The wound closure was photographed under phase-contrast microscopy. (B) The migration rate of U87 cells was assessed and UB significantly decreased the migration of U87 cells after 24 h in comparison to the control. (C) The mRNA expression of *VEGF* and *VEGFR* genes on U87 cells treated with 15 and 30 μM of UB was evaluated using qRT-PCR. The findings are demonstrated as means ± standard deviation (\*\* $p < 0.01$ , \*\*\* $p < 0.001$  contrasted with the control). UB, urolithin B

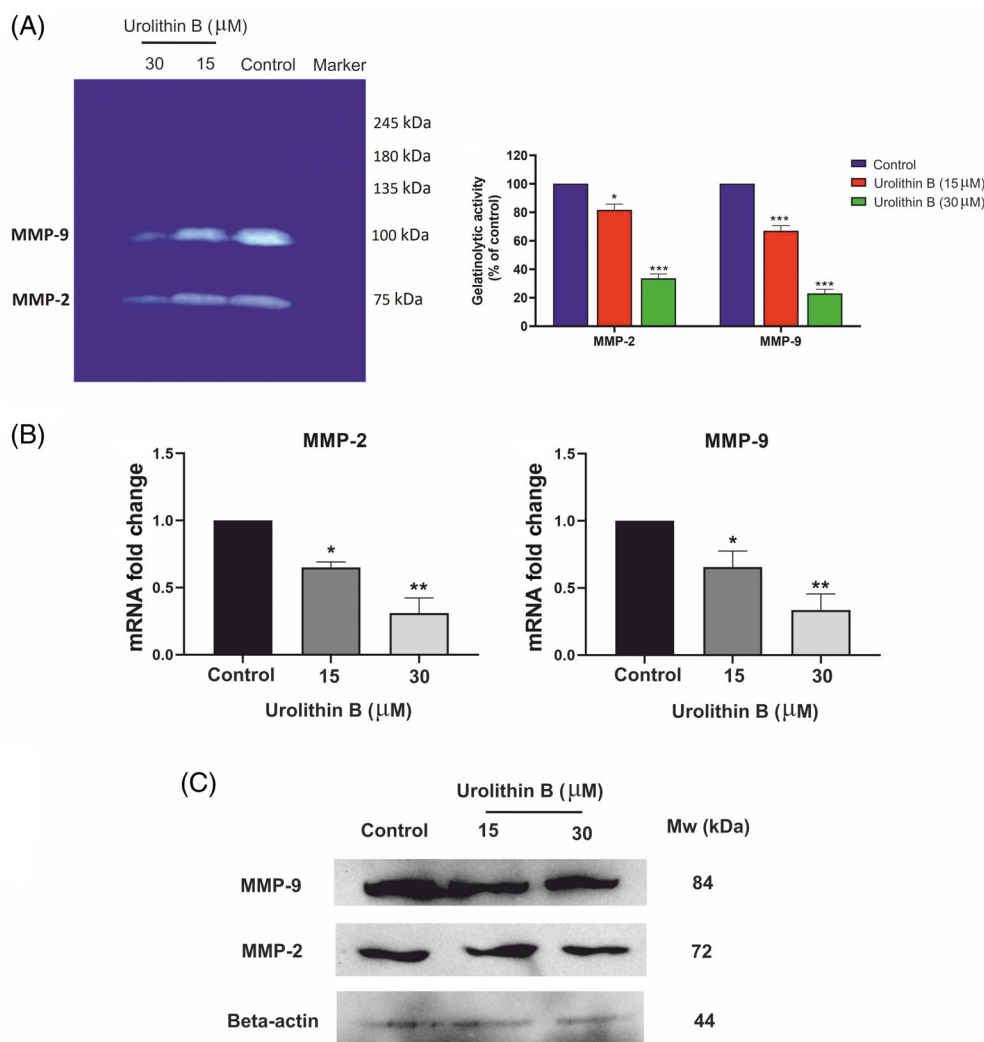


**FIGURE 6** (A) Effect of UB on MMP-2 and MMP-9 secretion and activity as measured by gelatin zymography in U87 cells. The cells were treated with UB (15 and 30  $\mu\text{M}$ ) for 24 h. The digested area of gelatine was quantified and represented as the mean  $\pm$  standard deviation of 3 independent tests. (B) The relative gene expression levels of MMP-2 and MMP-9 on U87 cells that have been treated with 15 and 30  $\mu\text{M}$  of UB after 24 h were evaluated using qRT-PCR. Data are represented as the mean  $\pm$  standard deviation and the levels of GAPDH in the samples were used to normalize the results. (C) the MMP-2 and MMP-9 protein expression in the U87 cell line was treated with UB (15 and 30  $\mu\text{M}$ ). The expression of MMP-2 and MMP-9 was analyzed using western blotting (\*\* $p < 0.001$ , \*\* $p < 0.01$ , and \* $p < 0.05$  contrasted with the control). UB, urolithin B

can be regulated by mitochondria.<sup>41</sup> During necrosis, Bcl-2 family members could interact with the components of the mitochondrial permeability transition pore (MPTP). Bax overexpression and Bcl-2 downregulation caused the prolonged opening of MPTP pores, MPTP-dependent mitochondrial swelling, loss of ATP production, and high ROS generation to ultimately mediate necrosis.<sup>41–43</sup>

Prior studies have noted the importance of using natural products as harmless chemotherapy compounds for cancer therapy.<sup>44</sup> The findings of the current research revealed that UB can reduce the viability of NIH/3T3 normal fibroblast and U87 GBM cell line, but higher  $\text{IC}_{50}$  for NIH/3T3 points out that UB is less harmful. This finding broadly supports the work of other studies showing that the viability of cancer cells was considerably reduced by UB and UA with less cytotoxicity toward normal cell lines.<sup>32,35,45</sup> González-Sarriás et al., showed that urolithins have neuroprotective effects and prevent  $\text{H}_2\text{O}_2$ -induced apoptosis in human SH-SY5Y neuron-like cells,

except for the lack of effect for UB.<sup>13</sup> This finding was also reported by DaSilva et al., who found that UA, UB, and their methylated derivatives mitigated  $\text{H}_2\text{O}_2$ -induced oxidative stress and apoptosis of SH-SY5Y neuron-like and murine BV-2 microglia cells.<sup>14</sup> UA and UB also decrease the LPS-induced inflammation in BV2 cells suggesting their potential neuroprotective effects.<sup>46</sup>

Recent research has revealed the broad heterogeneity of GBM cells, however, all of them can invade the surrounding tissue. Invasion and migration have been considered important obstacles to GBM therapy.<sup>47</sup> Thus, compounds that ameliorate invasion and tumor cell motility of GBM cells can be a good candidate to be used as drug intervention in patients with GBM.<sup>48</sup> The current study found that UB can significantly reduce the migration of U87 cells. Among the signaling pathways regulating GBM cell migration and metastasis, the hypoxia-inducible factor (HIF)-1/VEGF-A pathway is related to proliferation, cell survival, and migration principally through the VEGF-receptor (VEGFR).<sup>49</sup> However,



the qRT-PCR study failed to find any distinction in the mRNA expression of VEGF and VEGFR in control and UB-treated U87 cells. There are similarities between the attitudes expressed in this study and those described by Md Alaaddin et al., who reported that UA can significantly decreased wound healing migration of Cancer Cells.<sup>50</sup> Giménez-Bastida et al., also reported that a mixture of UA, UB, and EA significantly inhibited CCD18-Co colon fibroblast cells migration.<sup>51</sup>

It is believed that various extracellular matrix (ECM) components must be degraded for malignant neoplasms to invade. In reviewing the literature, more than 20 MMPs have been recognized as being responsible for degrading ECM, however, MMP-2 and MMP-9 are particularly connected to tumor invasion.<sup>52</sup> Wie Zhou et al., found that an increase in MMP-2 and MMP-9 expression is positively related to tumor grade, poor prognosis, and recurrent glioma.<sup>28</sup> Gelatin substrates and type IV collagen are degraded by MMP-2 and MMP-9, using gelatin zymography the activity and secretion of these two types of MMPs were evaluated on U87 cells treated with UB. It is interesting to note that UB could significantly decrease the activity of MMP-2 and MMP-9. A possible explanation for this might be that mRNA expression and protein levels of MMP-2 and MMP-9 reduced after treatments of U87 cells with UB. These results are consistent with other research findings indicating UA can decrease the MMP-9 activity in colorectal cancer cells.<sup>53</sup>

Although the current study found the anti-proliferative and anti-metastatic activity of the free form of UB, further in vivo and clinical trial research should be undertaken to investigate the anti-GBM activity after orally or intraperitoneally administration of urolithins (free or conjugated form) or ET-rich foods. Moreover, the pharmacokinetics and tissue distribution of urolithins after their direct intake have not been studied up to now, but there is evidence that showed intake of ET or EA-rich food products can be caused 14–25  $\mu$ M plasma levels of UA after 6–8 h of their intake.<sup>7,54</sup> Additionally, these data must be interpreted with caution because urolithins reach systemic tissues as conjugates rather than in their free form. Overall, further studies are needed to investigate the plasma concentration of the free and conjugated form of UB, to identify if conjugated UB can cross the blood–brain barrier, interact with neuronal cells, and also determine the underlying molecular mechanisms associated with the anti-metastatic and anti-proliferative effect of the free and conjugated form of UB.

## 5 | CONCLUSION

The current research is the initial investigation of UB's apoptotic and anti-metastatic effect on U87 GBM cells.

In summary, the current study's findings using in vitro analyses uncovered that UB induces ROS generation, necrosis, and G0/G1 cell cycle arrest in U87 cells. UB also caused down-regulation and up-regulation of Bcl2 and Bax apoptotic genes, respectively. Furthermore, according to these data, we can infer that UB effectively prevents the migration, invasion, and metastatic behavior of GBM cells by reducing the MMP-2 and MMP-9 enzymatic activities, and downregulating mRNA expression and protein levels of MMPs. After additional in vivo and mechanistic research on the free and conjugated form of UB, it may be regarded as a possible novel natural option for glioblastoma treatment because of its non-toxic nature, capacity to trigger necrosis and cell cycle arrest in U87 cells, and ability to inhibit metastasis.

## ACKNOWLEDGMENTS

None.

## CONFLICT OF INTEREST

The authors declare no conflict of interest to disclose.

## DATA AVAILABILITY STATEMENT

The data that support the findings of this study are available from the corresponding author upon reasonable request.

## ORCID

Fateme Eidizade  <https://orcid.org/0000-0002-3086-2678>

## REFERENCES

1. Donahue MJ, Blakeley JO, Zhou J, Pomper MG, Laterra J, Van Zijl PC. Evaluation of human brain tumor heterogeneity using multiple T1-based MRI signal weighting approaches. *Magn Reson Med*. 2008;59:336–44.
2. Weil RJ, Palmieri DC, Bronder JL, Stark AM, Steeg PS. Breast cancer metastasis to the central nervous system. *Am J Pathol*. 2005;167:913–20.
3. Johnson DR, O'Neill BP. Glioblastoma survival in the United States before and during the temozolomide era. *J Neurooncol*. 2012;107:359–64.
4. Cragg GM, Pezzuto JM. Natural products as a vital source for the discovery of cancer chemotherapeutic and Chemopreventive agents. *Med Princ Pract*. 2016;25(Suppl 2):41–59.
5. Huang Y, Hou Y, Qu P, Cai Y. Editorial: combating cancer with natural products: what would non-coding RNAs bring? *Front Oncol*. 2021;11:747586.
6. Giménez-Bastida JA, Ávila-Gálvez MÁ, Espín JC, González-Sarriás A. Evidence for health properties of pomegranate juices and extracts beyond nutrition: a critical systematic review of human studies. *Trends Food Sci Technol*. 2021;114:410–23.
7. Espín JC, Larrosa M, García-Conesa MT, Tomás-Barberán F. Biological significance of urolithins, the gut microbial ellagic acid-derived metabolites: the evidence so far. *Evid Based Complement Alternat Med*. 2013;2013:270418.

8. Hartman RE, Shah A, Fagan AM, Schweteye KE, Parsadanian M, Schulman RN, et al. Pomegranate juice decreases amyloid load and improves behavior in a mouse model of Alzheimer's disease. *Neurobiol Dis.* 2006;24:506–15.
9. Essa MM, Subash S, Akbar M, Al-Adawi S, Guillemin GJ. Long-term dietary supplementation of pomegranates, figs and dates alleviate neuroinflammation in a transgenic mouse model of Alzheimer's disease. *PLoS One.* 2015;10:e0120964.
10. Gasperotti M, Passamonti S, Tramer F, Masuero D, Guella G, Mattivi F, et al. Fate of microbial metabolites of dietary polyphenols in rats: is the brain their target destination? *ACS Chem Neurosci.* 2015;6:1341–52.
11. Kujawska M, Jourdes M, Kurpik M, Szulc M, Szafer H, Chmielarz P, et al. Neuroprotective effects of pomegranate juice against Parkinson's disease and presence of Ellagitannin-derived metabolite—Urolithin A—in the brain. *Int J Mol Sci.* 2020;21:202.
12. García-Villalba R, Giménez-Bastida JA, Cortés-Martín A, Ávila-Gálvez MÁ, Tomás-Barberán FA, Selma MV, et al. Urolithins: a comprehensive update on their metabolism, bioactivity, and associated gut microbiota. *Mol Nutr Food Res.* 2022; e2101019.
13. González-Sarriás A, Núñez-Sánchez MÁ, Tomás-Barberán FA, Espín JC. Neuroprotective effects of bioavailable polyphenol-derived metabolites against oxidative stress-induced cytotoxicity in human Neuroblastoma SH-SY5Y cells. *J Agric Food Chem.* 2017;65:752–8.
14. DaSilva NA, Nahar PP, Ma H, Eid A, Wei Z, Meschwitz S, et al. Pomegranate ellagitannin-gut microbial-derived metabolites, urolithins, inhibit neuroinflammation in vitro. *Nutr Neurosci.* 2019;22:185–95.
15. González-Sarriás A, Espín JC, Tomás-Barberán FA, García-Conesa MT. Gene expression, cell cycle arrest and MAPK signalling regulation in Caco-2 cells exposed to ellagic acid and its metabolites, urolithins. *Mol Nutr Food Res.* 2009;53:686–98.
16. Kasimsetty SG, Bialonska D, Reddy MK, Thornton C, Willett KL, Ferreira D. Effects of pomegranate chemical constituents/intestinal microbial metabolites on CYP1B1 in 22Rv1 prostate cancer cells. *J Agric Food Chem.* 2009;57:10636–44.
17. Adams LS, Zhang Y, Seeram NP, Heber D, Chen S. Pomegranate ellagitannin-derived compounds exhibit antiproliferative and antiaromatase activity in breast cancer cells in vitro. *Cancer Prev Res (Phila).* 2010;3:108–13.
18. Qiu Z, Zhou B, Jin L, Yu H, Liu L, Liu Y, et al. In vitro antioxidant and antiproliferative effects of ellagic acid and its colonic metabolite, urolithins, on human bladder cancer T24 cells. *Food Chem Toxicol.* 2013;59:428–37.
19. Präbst K, Engelhardt H, Ringgeler S, Hübner H. Basic colorimetric proliferation assays: MTT, WST, and Resazurin. *Methods Mol Biol.* 2017;1601:1–17.
20. Jalili-Nik M, Abbasinezhad-Moud F, Sahab-Negah S, Maghrouni A, Etezad Razavi M, Khaleghi Ghadiri M, et al. Antitumor effects of 5-Aminolevulinic acid on human malignant glioblastoma cells. *Int J Mol Sci.* 2021;22:5596.
21. Jalili-Nik M, Sadeghi MM, Mohtashami E, Mollazadeh H, Afshari AR, Sahebkar A. Zerumbone promotes cytotoxicity in human malignant glioblastoma cells through reactive oxygen species (ROS) generation. *Oxid Med Cell Longev.* 2020;2020:3237983–9.
22. Lyublinskaya OG, Ivanova JS, Pugovkina NA, Kozhukharova IV, Kovaleva ZV, Shatrova AN, et al. Redox environment in stem and differentiated cells: a quantitative approach. *Redox Biol.* 2017;12:758–69.
23. Sahab-Negah S, Ariakia F, Jalili-Nik M, Afshari AR, Salehi S, Samini F, et al. Curcumin loaded in Niosomal nanoparticles improved the anti-tumor effects of free curcumin on glioblastoma stem-like cells: an In vitro study. *Mol Neurobiol.* 2020;57:3391–411.
24. Jalili-Nik M, Afshari AR, Sabri H, Bibak B, Mollazadeh H, Sahebkar A. Zerumbone, a ginger sesquiterpene, inhibits migration, invasion, and metastatic behavior of human malignant glioblastoma multiforme in vitro. *Biofactors.* 2021;47:729–39.
25. Afshari AR, Jalili-Nik M, Soukhtanloo M, Ghorbani A, Sadeghnia HR, Mollazadeh H, et al. Auroptene-induced cytotoxicity mechanisms in human malignant glioblastoma (U87) cells: role of reactive oxygen species (ROS). *EXCLI J.* 2019;18:576–90.
26. Poonaki E, Ariakia F, Jalili-Nik M, Shafiee Ardestani M, Tondro G, Samini F, et al. Targeting BMI-1 with PLGA-PEG nanoparticle-containing PTC209 modulates the behavior of human glioblastoma stem cells and cancer cells. *Cancer Nanotechnol.* 2021;12:5.
27. Zhang L, Wang JN, Tang JM, Kong X, Yang JY, Zheng F, et al. VEGF is essential for the growth and migration of human hepatocellular carcinoma cells. *Mol Biol Rep.* 2012;39:5085–93.
28. Zhou W, Yu X, Sun S, Zhang X, Yang W, Zhang J, et al. Increased expression of MMP-2 and MMP-9 indicates poor prognosis in glioma recurrence. *Biomed Pharmacother.* 2019;118:109369.
29. Wirsching HG, Galanis E, Weller M. Glioblastoma. *Handb Clin Neurol.* 2016;134:381–97.
30. Demain AL, Vaishnav P. Natural products for cancer chemotherapy. *J Microbial Biotechnol.* 2011;4:687–99.
31. Al-Harbi SA, Abdulrahman AO, Zamzami MA, Khan MI. Urolithins: the gut based polyphenol metabolites of Ellagitannins in cancer prevention, a review. *Front Nutr.* 2021;8:647582.
32. Lv MY, Shi CJ, Pan FF, Shao J, Feng L, Chen G, et al. Urolithin B suppresses tumor growth in hepatocellular carcinoma through inducing the inactivation of Wnt/ $\beta$ -catenin signaling. *J Cell Biochem.* 2019;120:17273–82.
33. Kasimsetty SG, Bialonska D, Reddy MK, Ma G, Khan SI, Ferreira D. Colon cancer chemopreventive activities of pomegranate ellagitannins and urolithins. *J Agric Food Chem.* 2010;58:2180–7.
34. Liou GY, Storz P. Reactive oxygen species in cancer. *Free Radic Res.* 2010;44:479–96.
35. El-Wetidy MS, Ahmad R, Rady I, Helal H, Rady MI, Vaali-Mohammed MA, et al. Urolithin a induces cell cycle arrest and apoptosis by inhibiting Bcl-2, increasing p53-p21 proteins and reactive oxygen species production in colorectal cancer cells. *Cell Stress Chaperones.* 2021;26:473–93.
36. Gottlieb E, Vander Heiden MG, Thompson CB. Bcl-x (L) prevents the initial decrease in mitochondrial membrane potential and subsequent reactive oxygen species production during tumor necrosis factor alpha-induced apoptosis. *Mol Cell Biol.* 2000;20:5680–9.
37. Cadenas E. Mitochondrial free radical production and cell signaling. *Mol Aspects Med.* 2004;25:17–26.



38. Naseri MH, Mahdavi M, Davoodi J, Tackallou SH, Goudarzvand M, Neishabouri SH. Up regulation of Bax and down regulation of Bcl2 during 3-NC mediated apoptosis in human cancer cells. *Cancer Cell Int.* 2015;15:55.
39. Dejean LM, Martinez-Caballero S, Guo L, Hughes C, Teijido O, Ducret T, et al. Oligomeric Bax is a component of the putative cytochrome c release channel MAC, mitochondrial apoptosis-induced channel. *Mol Biol Cell.* 2005;16:2424–32.
40. Zhou B, Wang J, Zheng G, Qiu Z. Methylated urolithin a, the modified ellagitannin-derived metabolite, suppresses cell viability of DU145 human prostate cancer cells via targeting miR-21. *Food Chem Toxicol.* 2016;97:375–84.
41. Karch J, Molkentin JD. Regulated necrotic cell death. *Circ Res.* 2015;116:1800–9.
42. Marzo I, Brenner C, Zamzami N, Jürgensmeier JM, Susin SA, Vieira HL, et al. Bax and adenine nucleotide translocator cooperate in the mitochondrial control of apoptosis. *Science (New York, NY).* 1998;281:2027–31.
43. Shimizu S, Eguchi Y, Kamiike W, Funahashi Y, Mignon A, Lacronique V, et al. Bcl-2 prevents apoptotic mitochondrial dysfunction by regulating proton flux. *Proc Natl Acad Sci U S A.* 1998;95:1455–9.
44. Lin SR, Chang CH, Hsu CF, Tsai MJ, Cheng H, Leong MK, et al. Natural compounds as potential adjuvants to cancer therapy: preclinical evidence. *Br J Pharmacol.* 2020;177:1409–23.
45. González-Sarrías A, Tomé-Carneiro J, Bellesia A, Tomás-Barberán FA, Espín JC. The ellagic acid-derived gut microbiota metabolite, urolithin a, potentiates the anticancer effects of 5-fluorouracil chemotherapy on human colon cancer cells. *Food Funct.* 2015;6:1460–9.
46. Xu J, Yuan C, Wang G, Luo J, Ma H, Xu L, et al. Urolithins attenuate LPS-induced Neuroinflammation in BV2 Microglia via MAPK, Akt, and NF- $\kappa$ B signaling pathways. *J Agric Food Chem.* 2018;66:571–80.
47. Lah TT, Novak M, Breznik B. Brain malignancies: glioblastoma and brain metastases. *Semin Cancer Biol.* 2020;60:262–73.
48. Wells A, Grahovac J, Wheeler S, Ma B, Lauffenburger D. Targeting tumor cell motility as a strategy against invasion and metastasis. *Trends Pharmacol Sci.* 2013;34:283–9.
49. Onishi M, Kurozumi K, Ichikawa T, Date I. Mechanisms of tumor development and anti-angiogenic therapy in glioblastoma multiforme. *Neurol Med Chir.* 2013;53:755–63.
50. Alauddin M, Okumura T, Rajaxavier J, Khozoei S, Pöschel S, Takeda S, et al. Gut bacterial metabolite Urolithin a decreases Actin polymerization and migration in cancer cells. *Mol Nutr Food Res.* 2020;64:e1900390.
51. Giménez-Bastida JA, Larrosa M, González-Sarrías A, Tomás-Barberán F, Espín JC, García-Conesa MT. Intestinal ellagitannin metabolites ameliorate cytokine-induced inflammation and associated molecular markers in human colon fibroblasts. *J Agric Food Chem.* 2012;60:8866–76.
52. Devy L, Dransfield DT. New strategies for the next generation of matrix-metalloproteinase inhibitors: selectively targeting membrane-anchored MMPs with therapeutic antibodies. *Biochem Res Int.* 2011;2011:191670.
53. Zhao W, Shi F, Guo Z, Zhao J, Song X, Yang H. Metabolite of ellagitannins, urolithin a induces autophagy and inhibits metastasis in human sw620 colorectal cancer cells. *Mol Carcinog.* 2018;57:193–200.
54. Cerdá B, Espín JC, Parra S, Martínez P, Tomás-Barberán FA. The potent in vitro antioxidant ellagitannins from pomegranate juice are metabolised into bioavailable but poor antioxidant hydroxy-6H-dibenzopyran-6-one derivatives by the colonic microflora of healthy humans. *Eur J Nutr.* 2004;43:205–20.

**How to cite this article:** Eidizade F, Soukhtanloo M, Zhiani R, Mehrzad J, Mirzavi F. Inhibition of glioblastoma proliferation, invasion, and migration by Urolithin B through inducing G0/G1 arrest and targeting MMP-2/-9 expression and activity. *BioFactors.* 2023;49(2):379–89. <https://doi.org/10.1002/biof.1915>